STUDY OF TOTAL SOLAR IRRADIANCE TIME SERIES USING CHAOTIC AND WAVELET POWER SPECTRUM ANALYSIS

Supported by tetfund TERTIARY EDUCATION TRUST FUND

A. D. Adelaja[1&2]*, J. A. Laoye[2], R. K. Odunaike[2], E. O. Falayi[1], Q. A. Adeniji[3] and F. O. Ogunsanwo[1]
[1]Department of Physics, Tai Solarin University of Education, Ijagun, Ijebu-Ode, Nigeria
[2]Statistical and Nonlinear Physics Research Group, Department of Physics, Olabisi Onabanjo University, Ago-Iwoye, Nigeria
[3]Department of Physics, Federal University Kashere, Nigeria
*Correspondence: ayodeleenochadelaja@gmail.com

Received: February 21, 2021 **Accepted:** June 15, 2021

Abstract: This study reported the analyses of daily–recorded variability of the Total Solar Irradiance (TSI) (daily means) measurements using chaos theory such as mutual information, false nearest neighbours (FNN), Lyapunov exponent, phase space reconstruction and power spectrum. In an attempt to identify the temporal correlation of the TSI data, Space- time separation plots were also analysed. Wavelet power spectrum (WPS) which splits the time series into different scales and monitors energy distribution in each scale was also computed. Our analyses revealed that FNN had its first at an embedding dimension of four. The phase space reconstruction for TSI time series using time delay embedding for $\tau = 15$ and $m = 4$ was also reported. The power spectrum calculated was broadband in nature and also decays exponentially, an indication of the possibility of chaotic behaviour. Analysis of space- time separation plot for TSI time series shows oscillations covering a small scale range and as such there is no prominent temporal correlation in the data. The divergence in the trajectories of TSI data as given by largest Lyapunov exponent curve indicated a very strong possibility of chaos. WPS analysis reveals the multi-scale and non-stationary behaviour of the data with greater concentration of power between 1024 and 204 minutes bands. Sequel to all analyses conducted, it could be inferred that TSI data could be modeled and predicted with a minimum of four dynamical variables since the first minimum of the false nearest neighbours plot occurred at an embedding dimension of four.

Keywords: Total solar irradiance, false nearest neighbours, chaotic quantifier

Introduction

Earth's climatic system is driven by solar energy and this energy has potential to directly alter the climate (Falayi *et al*., 2020). Sun as a complex system has its energy varying due to spatial and temporal variability of large scale magnetic structure and fluctuation in the activity of the Sun has been given as the major factors contributing to the great variation in Earth's climate system (Falayi *et al*., 2020; Haigh, 2003; Lean, 2006; Gray *et al*., 2010). According to Gray *et al*. (2010) and Lockwood (2010), Total Solar Irradiance (TSI) is regarded as the most obvious and least controversial mechanism for the sun to influence the climate. Total solar irradiance is the amount of radiant energy emitted by the sun over all wavelengths that fall each second on 11 feet square (1 m^2) above Earth's surface. Analyzing and predicting solar irradiance is of great importance because it has so many applications, which includes energy generation for solar based power plants. The constraints in having exact effect of the role of Sun in recent global warming and its projections for future influence in the area of man-made climate change is as a result the uncertainty in solar variability, Adewole *et al*. (2020). The cause for this variability has been temporal over the century while different approaches have been taken at reconstructing the total solar irradiance employing a substantial degree of empiricism, Falayi *et al*. (2020). Several research works had been carried out on variability of total solar irradiance but statistical approaches were mostly adopted to analyse the time series pertaining weather and environment related issue, these approaches were majorly based upon some tacit assumptions, such assumptions could sometimes lead to wrong conclusions especially if the underlying processes are complex and not linear or if highly dynamic in nature. Various fields are now adopting the use of nonlinear chaotic techniques due to their relevant mathematical approach that are useful in identifying and quantifying the nonlinear fluctuations in time-series data. From the available empirical works of Rabiu *et al*. (2014); Ogunsua *et al*. (2014) and Oludehinwa *et al*. (2014), all used chaotic techniques to study the dynamics of ionospheric and magnetospheric. Chaotic techniques had also been used in prediction of sunspot (Gkana and Zachilas, 2015; Sarp *et al*., 2018) and as well in climate and weather forecast (Sharma and Veeramani, 2011; Fuwape *et al*., 2016). TSI dynamics are governed by these various physical mechanisms which are acting on a range of temporal and spatial scales. To the best knowledge of the researchers, no extensive study on the chaotic nature of the solar irradiance and this motivated the current study to ascertain the variabilities and unravel the chaotic nature of the total solar irradiance thereby studying the total solar irradiance time series.

Materials and Methods

The data used were provided by the Active Cavity Radiometer Irradiance Monitor (ACRIM II) on the Upper Atmosphere Research Satellite (UARS) spacecraft (http://www.acrim.com/). The data set measured at1 Astrological Unit- A.U. (Watts/meters-squared) was displayed as the daily means –recorded variability of the total solar irradiance with temporal coverage from 4th October, 1991 to 1st November, 2001. Analyzing the chaoticity of TSI time series, nonlinear techniques such as average mutual information (AMI), false nearest neighbour (FNN), phase space construction and the estimation of other chaotic quantifiers: Lyapunov exponent and power spectrum were employed. A suitable embedding dimension (m) that is needed to reconstruct phase space was obtained. Phase spaces reconstructions structure could be described by the embedding dimension as it was obtained from the variations in the coordinates by applying delay dimension as this explains its time evolution.

Results and Discussion

Nonlinear time series analysis

A nonlinear technique and wavelet spectrum methods are employed to study time series of TSI data in the course of investigating the dynamics and energy distribution of the data. A time series is repeated measurements of a single variable in which the measured single variable may be as a result of some hidden underlying variables. Fig. 1 is the time series for the TSI data, here the variability of the point plotted are

characterized with high level of fluctuations showing that the system does not show any regular patterns. These irregular patterns make the description of the internal dynamics difficult; hence it is important to subject the data to some nonlinear technique in order to unravel the system internal dynamics.

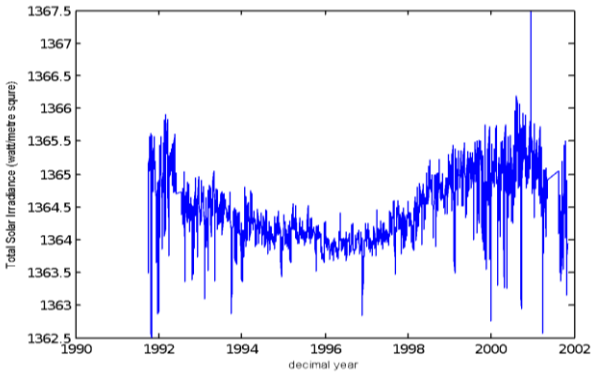

Fig. 1: Time series of Total Solar Irradiance data from 4th October, 1991 to 1st November, 2001

Revealing the multidimensional phase space of such system (time series) without prior knowledge of the number of variables of the system becomes problematic. The chaoticity and dynamical complexity of such system are nonlinear phenomena which that describe the state of some dynamical systems. This difficulty can be overcome by adopting nonlinear time series technique. Nonlinear time-series analysis consists of different set of methods that reveal dynamical information about the next set of values in a data set. This background nonlinear time-series analysis critically based on the concept of re-construction of the state space of the system where the data are sampled (Takens, 1981).

Average mutual information (AMI) technique

In reconstructing the attractor of TSI data successfully using equation (1), appropriate values for τ is required and according to Shaw (1981), the value is given as the first minimum of AMI (I (τ)). Fraser and Swinney (1986) explained the concept of mutual information between x_i and $x_{i+\tau}$ as a suitable measure for determining delay time (τ). The mutual information between x_i and $x_{i+\tau}$ provides the amount of information anyone would have about the state $x_{i+\tau}$ presuming state x_i is known already.

Having a time series of the form $\{x_0, x_1, x_3, ...x_1, x_2, ...x_i, ...x_n\}$, the first step is to determine the minimum ($x_{\min}$) and the maximum ($x_{\max}$) of the sequence after which the absolute value of the difference $|x_{\max} - x_{\min}|$ is taken and then partitioned into j equally sized intervals, where j is a large enough integer number as indicated in the expression in equation (1).

$$I(\tau) = -\sum_{q=1}^{j}\sum_{r=1}^{j} p_{qr}(\tau)\ln\frac{p_{qr}(\tau)}{p_q p_r} \qquad (1)$$

Where p_q and p_r denote the probabilities that the variable assumes a value inside the q[th] and *r*[th] bins respectively, and $p_{qr}(\tau)$ is the joint probability that x_i is in bin q and $x_{i+\tau}$ is in bin r.

Figure 2 shows the variation of average mutual information plotted against the delay time and it was observed that for all the daily TSI time series, the choice of $\tau \geq 15$ is appropriate since the mutual information has the first minimum at about τ = 15. Based on this result, it is evident that a delay time of 15 is adequate to calculate the largest Lyaponuv exponent which reveals whether the system is chaotic or otherwise.

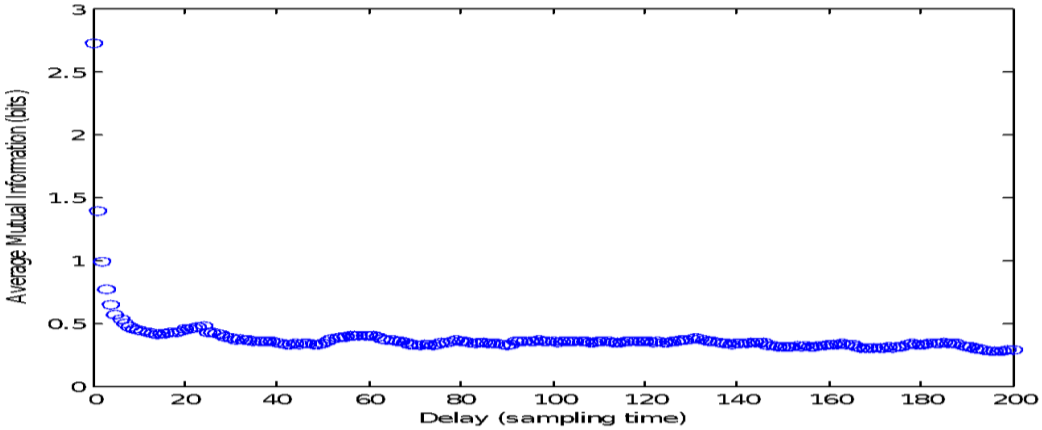

Fig. 2: Variation of mutual information against time delay as obtained from the time series of TSI data between 4th October, 1991 and 1st November, 2001having the first minimum of delay time (τ) at about 15

False nearest neighbour (FNN) determination

Wallot and Monster (2018) suggested that one of the effective methods to determine the embedding dimension from the phase space reconstruction is the false nearest neighbour method (FNN). The FNN algorithm is based on the geometry of the phase space reconstructed using a single time series. The major concept is to investigate how the number of FNN changes along the trajectory with increase in embedding dimension. The FNN method relies on the assumption that an attractor of a deterministic system folds and unfolds smoothly with no sudden irregularities in its structure. Therefore, points that are close in the reconstructed embedding space have to stay sufficiently close also during forward iteration. Satisfying this criterion, then under some sufficiently short forward

iteration the distance between two points p(i) and p(j) of the reconstructed attractor, which are initially only a small ε apart, cannot grow further as $R_{tr}\varepsilon$, where R_{tr} is a given constant. However, if an i^{th} point has a close neighbour that does not fullfil this criterion, then this i^{th} point is marked as having a false nearest neighbour. Choosing a sufficiently large m minimizes the fraction of points having a false nearest neighbour but if m is too small, then two points of the attractor may solely appear to be close, whereas under forward iteration they are mapped randomly due to projection effects. The random mapping occurs because the whole attractor is projected onto a hyper plane that has a smaller dimensionality than the actual phase space and so the distances between points become distorted. In order to obtain the fraction of false nearest neighbours, given a point p(i) in the m-dimensional embedding space, there is need to determine a neighbour p(j), so that $\|p(i)-p(j)\|<\varepsilon$, where ‖⋯‖ is the square norm and ε is a small constant usually not larger than the standard deviation of data. Normalized distance R_i between the $(m+1)^{th}$embedding coordinate of points p(i) and p(j) is calculated according to equation (2):

$$R_i = \left| \frac{x_{i+mx} - x_{j+mx}}{\left\| p_{(i)} - p_{(j)} \right\|} \right| \quad (2)$$

If R_i is larger than a given threshold R_{tr}, then p(i) is marked a shaving a false nearest neighbour. Equation (2) has to be applied for the whole time series and for various m = 1,2, until the fraction of points for which $R_i > R_{tr}$ is negligible. Here, FNN algorithm was applied on the total solar irradiance time series and the variation of the fraction of false nearest neighbours for different embedding dimensions was shown in Fig. 3. It can be seen that the fraction of nearest neighbours was falling to its first minimum value at an embedding dimension of 4. This indicated that minimum of four dynamical variables will be sufficient to model and explain the dynamics of total solar irradiance time series.

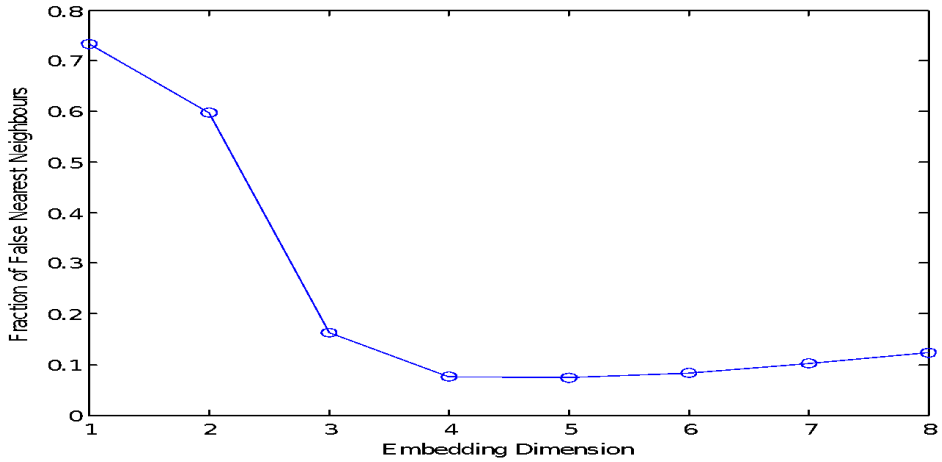

Fig. 3: Fraction of false nearest neighbours for the time series of total solar irradiance between 4th October, 1991 and 1st November, 2001showing its first minimum at m = 4

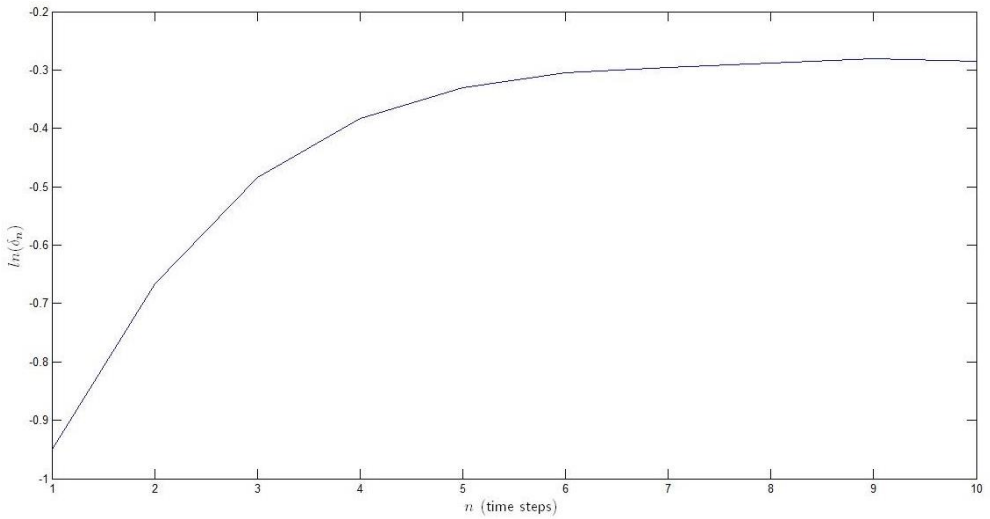

Fig. 4: Lyapunov exponent and its evolution, computed as the state space trajectory with τ = 15and m = 4

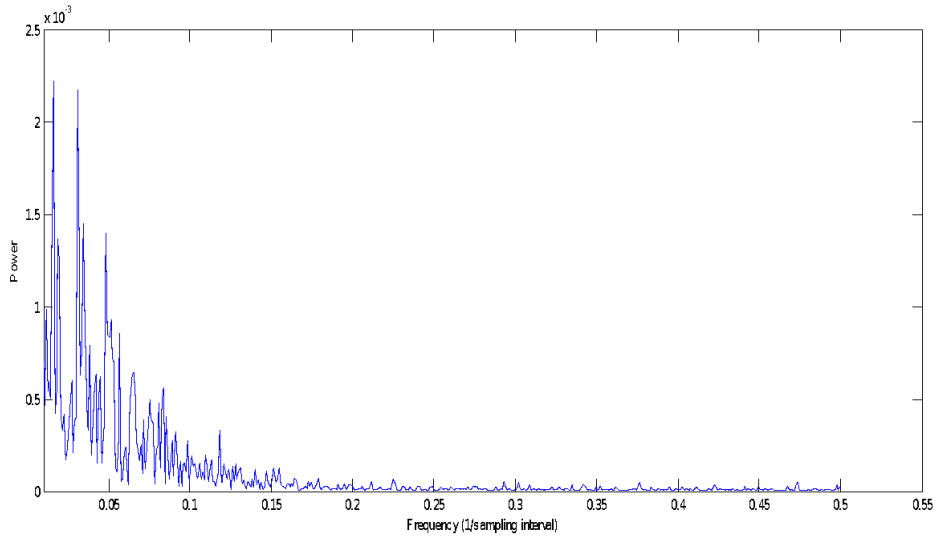

Fig. 5: The power spectrum of time series of total solar irradiance between 4th October, 1991 and 1st November, 2001

Chaotic quantifiers: Lyapunov exponents and power spectrum

The Lyapunov exponent is an important chaotic quantifier that indicates divergence of trajectory in one dimension. It can also be regarded as a repulsion or attraction from a fixed point. The possibility of presence of chaos in a dissipative system is when its Lyapunov exponent has a positive value. In 3 or more dimensional systems, the largest Lyapunov exponent (λ_1) can be used to determine the rate of its divergence (Wolf *et al.*, 1985) and the expression is given as:

$$\lambda_1 = \underset{r\to\inf}{Lim}\frac{1}{t}\log\frac{\Delta x(t)}{x(0)} = \underset{r\to\inf}{Lim}\frac{1}{t}\sum_{i=1}^{t}\log\frac{\Delta x(t_i)}{\Delta x(t_{i-1})} \quad (3)$$

The Lyapunov exponent was estimated for TSI data and its evolution in state space was obtained with τ = 15, m = 4, as depicted in Fig. 4. Having observed that the exponential graph shows the divergence of the data as time evolves which is a strong indication of the possibility of the system being chaotic, another chaotic quantifier called power spectrum was also carried out. The power spectrum of the time series of TSI as depicted in Fig. 5 shows a broadband nature and also exponentially decay which removes the likelihood of possibility of random behavior and thus, indicates the chaotic behaviors of the TSI time series.

Phase space reconstruction

An approach in which a single variable series is reconstructed in a multi-dimensional phase space to reveal the crucial dynamical properties of the underlying system is referred to as phase space reconstruction. This method uses the concept of reconstruction of a single-variable past history (time series) and a method of delays in a multi-dimensional phase space to represent the underlying dynamics. The phase space is reconstructed by taking the time series as X_1, X_2, X_3,...X_N and creating D-dimensional vectors using a time delay τ. The techniques of delays are applied to reconstruct phase space and this can be the most significant in phase space reconstruction system. With the aid of embedding theorem, the phase space reconstruction that helped to identify the multidirectional state was realized (Takens, 1981) and given as follows:

$$p(i) = (x_i, x_{i+\tau}, x_{i+2\tau}, \ldots\ldots\ldots, x_{i+(m-1)\tau}) \quad (4)$$

Where p(i) are vectors in phase space, τ and m are the time delay and the embedding dimension respectively.

Takens (1981) reported that for a large enough m, this procedure, known as delay coordinate embedding, provides a one-to-one image of the original system. In other words, the attractor constructed according to equation (4) will have the same mathematical properties, such as the dimension, Lyapunov exponents, etc as the original system. According to Abarbanel (1996), the key to understanding lies in the fact that all variables in a nonlinear process are generically connected (influence one another). Thus, every subsequent point of a given measurement x_i is the result of an entangled combination of influences from all other system variables. Accordingly, $x_{i+\tau}$ may be viewed as a substitute second system variable, which carries information about the influences of all other variables during time τ. Having this in mind, one can introduce the 3rd ($x_{i+2\tau}$), 4th ($x_{i+3\tau}$),...,m^{th} ($x_{i+(m-1)\tau}$) substituting variable, and thus obtain the whole m dimensional phase space where the substitute variables incorporate all influences of original system variables, provided m in equation(4) is large enough. To reveal the multidimensionality of TSI data, delay dimension was applied on the data and the reconstructed phase space trajectory was shown in Fig. 6.

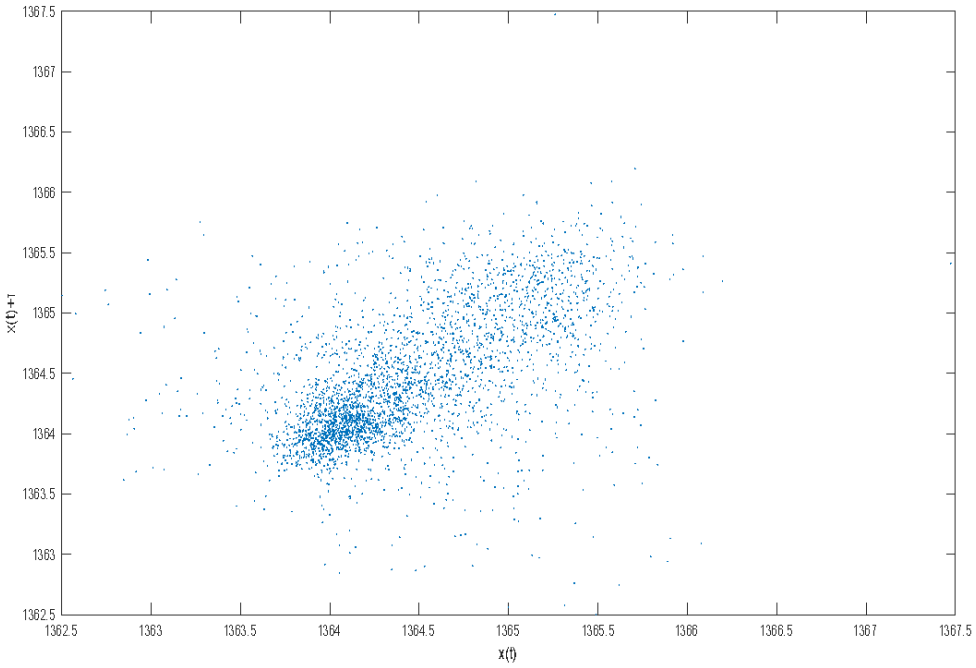

Fig. 6: Delay representation of the reconstructed phase space for the time series of total solar irradiance between 4th October, 1991 and 1st November, 2001

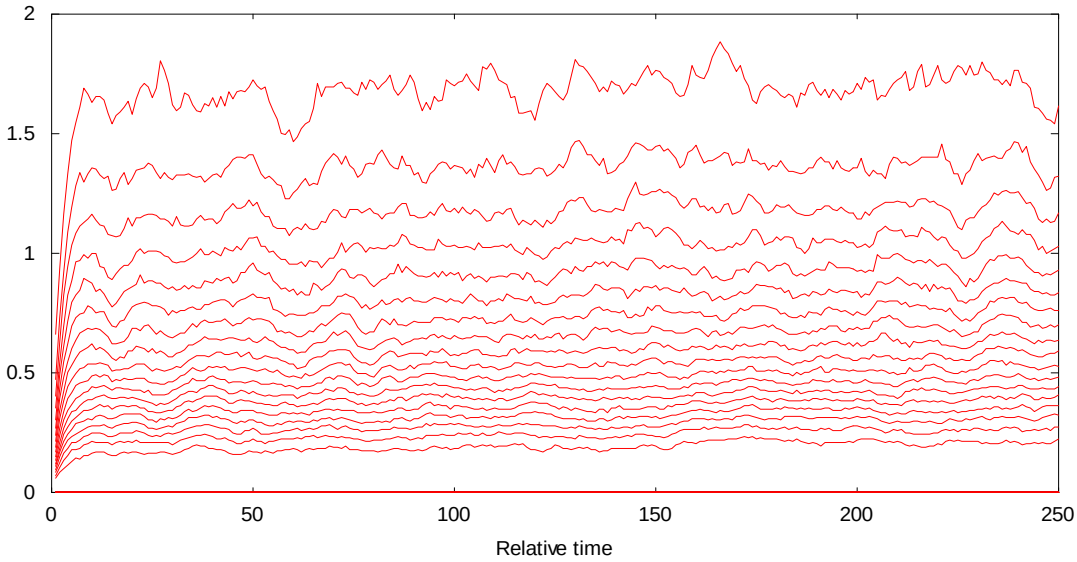

Fig. 7: Space-time separation plot for the time series of total solar irradiance between 4th October, 1991 and 1st November, 2001

Space-time separation plot

Theiler (1991) opined that if temporal correlation is present in a time series, it may result into pseudo estimation of the correlation dimension of the attractor. Removing the pseudo effect, the temporally correlated points from the pair counting in the correlation sum should be taken away. To identify the temporal correlation of the data, a stationarity test called space–time separation plot is required. The most common definition of a stationarity process is that, all conditional probabilities are constant in time. The interdependence existing in a system can be detected by plotting the number of pairs of points as a function of the two variables, namely, the time separation D_t, and the spatial distance, (Provenzale *et al*., 1992). Fig. 7 is the space-time separation plot of the TSI data where it can be seen that the curves exhibit small scale oscillations and as such temporal correlation in the data was not prominent in the data.

Wavelet power spectrum analysis (WPS)

WPS is an important technique that reveals the localized variations of power in a given time series. It is a mathematical tool that is useful for investigating time series with different scales (Liu and Babanin, 2004; Zossi *et al*., 2008). Falayi *et al*. (2020) explained that WPS is produced by an enlargement of $\psi(t) \rightarrow \psi(t)$ with further projection $\psi(t) \rightarrow \psi(t+1)$ with respect to time *t*. Equation (5) expresses the mother wavelet.

$$\psi_{a,b}(t) = a^{\frac{1}{2}}\psi\left(\frac{t-b}{a}\right) \quad (5)$$

Where *a* is the scale or dilation of the wavelet and b is the translation or position (time localization).

Torrence and Compo (1998) expresses equation (6) as Morlet wavelet

$$\psi(t) = \frac{e^{i\omega_0 t}}{\sqrt[4]{\pi e^{\frac{t^2}{2}}}} \quad (6)$$

Where ω_0 is the dimensionless frequency called wave number.

The application of WPS on *S(n)* time series is termed the convolution of the data series of the Morlet wavelets and is expressed as equation (7)

$$WPS(a,b) = \int_{-\infty}^{\infty} s(n)\psi^{*}{}_{a,b}(t)dt \quad (7)$$

Where $\psi^{*}{}_{a,b}(t)$ is the conjugate of the wavelet function $\psi_{a,b}(t)$. Equation (8) gives the expression of the mother wavelet in terms of the wavelet coefficient at time index n and scale *a*.

$$WPS_n(a) = \sum_{n^l=0}^{N-1} s(n^l)\psi^{*}\left[\frac{(n^l-n)\,dt}{a}\right] \quad (8)$$

The length of the data in the time series is represented as N while *dt* represents the time interval.

Investigation of the variation in power over a band of scales is given by the scale-averaged WPS expressed in Equation (9) as stated in Torrence and Compo (1998):

$$\overline{W_{n^{\backslash}}{}^2} = \frac{\partial j \partial t}{0.776}\sum_{j=j1}^{j^2}\frac{\left|W(a_j)\right|^2}{a_j} \quad (9)$$

In order to identify the highest energetic phase that is associated with the cross-wavelet analysis, global wavelet spectrum (GWS) with expression given in equation (10) was employed.

$$GSW = \int \left|WPS(a,b)\right|^2 db \quad (10)$$

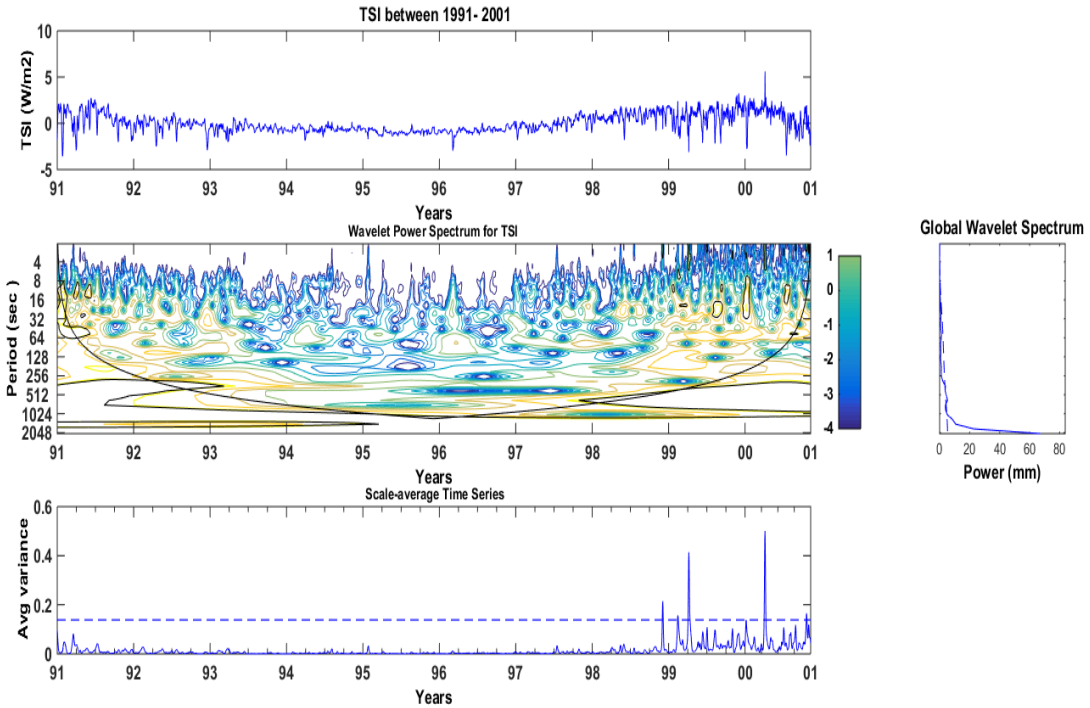

Fig. 8: (a) Time series of TSI data from 4th October, 1991 to 1st November, 2001 (b) The WPS for TSI data, concentration of power is between the 1024 and 204 min bands. (c) The GWS which indicates dominant periods of the signals of the TSIdata, while the breaking lines symbolize significance level of 5% (d). The breaking lines in scale-average time series symbolize confidence level of 95% of the TSI data

To examine the solar activity, the time series of the TSI was shown in Fig. 8 (a-d). Fig. 8(a) shows the raw data of the TSI from 1991 to 2001 and Fig. 8(b) shows the power (absolute value squared) of the wavelet transform for the TSI. This value gives information on the relative power at a certain scale and a certain time. The power concentration can simply be recognized in the frequency or time domain. The colour bars of the WPS range from blue (low power) to red (high power), and the significant regions are the ones associated with red, orange, and yellow, right display the numerical strength of coupling between two variables. The annual frequency can be observed from 1991 to 2001 with power reduction from 1991 to 1998. The cross-hatched region in this Figure 8(b) is the cone of influence, where zero padding has reduced the variance. It was observed that there is a greater concentration of power between the 1024 and 204 min bands,

which indicated that this time series has a strong annual signal of TSI(Figure 8(b)). The GWS in Fig. 8(c) was used to study the dominant periods of the signals of the TSIdata for the different conditions during the year under while Fig. 8(d) is the Scale-average time series of the power wavelet over the 1024 and 204 min bands, the dashed line signifies the 95% confidence.

Conclusion

This study identified the existence chaos within the time series of total solar irradiance data from 4th October, 1991 to 1st November, 2001. Non-linear aspects such as mutual information, fraction of false nearest neighbours, phase space reconstruction and power spectrum were used to determine the chaotic behaviour of concerned system. Lyapunov exponent as a significant chaotic quantifier was estimated. Space - time separation plots was also conducted on the time series of total solar irradiance data. Wavelet power spectrum (WPS) analysis helps in reducing time series of TSI data into different scales. Sequel to all the analysis conducted, it could be inferred that total solar irradiance data could be modelled with a minimum of four dynamical variables since the fraction of false nearest neighbours analysis of the time series had its first minimum at an embedding dimension of four. The power spectrum calculated is broadband in nature and decays exponentially, an indication of the possibility of chaotic behaviour. Space- time separation plots for the time series exhibited small scale oscillations, and temporal correlation in the data was not prominent. The reconstructed phase space for the total solar irradiance time series using time delay embedding for $\tau = 15$ and $m = 4$, indicated the divergence of the trajectories which is a strong evidence of the presence of chaos. Finally, WPS reveals that there was a greater concentration of power between 1024 and 204 min bands.

.

Acknowledgement

Authors appreciate the technical assistance of the Atmospheric Science Data Centre (ASDC) (http://eosweb.larc.nasa.gov/DATADOCS/web_order.html) for granting them access to the Total Solar Irradiance mean daily data.

Conflict of Interest

The authors declare that there is no conflict of interest reported in this work.

References

Abarbanel HDI 1996. Analysis of Observed Chaotic Data. New York: Springer, ISBN: 978-1-4612-0763-4 (on line), pp: 13 - 93.

Adewole AT, Falayi EO, Roy-Layinde TO & Adelaja AD 2020. Chaotic Time Series analysis of meteorological parameters in some selected stations in Nigeria. *Scientific African*. doi: https://doi.org/10.1016/j.sciaf.2020.e00617

Falayi EO, Adewole AT, Adelaja AD, Ogundile OO & Roy-Layinde TO 2020. Study of nonlinear time series and wavelet power spectrum analysis using solar wind parameters and geomagnetic indices. *NRIAG J. Astron. and Geophys.*, 9(1): 226-237.

Fraser AM & Swinney HL 1986Independent coordinates for strange attractors from mutual information. *Phys. Rev.* A, 33(2): 1134–1140.

Fuwape IA, Ogunjo ST, Oluyamo SS, Rabiu AB 2016. Spatial variation of deterministic chaos in mean daily temperature and rainfall over Nigeria. *Theor. Appl. Climatol*. Doi:10.1007/s00704-016-1867-x

Gkana A & Zachilas L 2015. Sunspot numbers: data analysis, predictions and economic impacts. *J. Engr. Sci. Tech. Rev.*, 8(1):79–85.

Gray LJ, Beer J, Geller M, Haigh J, Lockwood M, Mathes K, Cubasch U, Fleitmann D, Harrison G, Hood L, Luterbacher J, Marsh N, Shindell D, Van Geel B & White W 2010. Solar influences on climate. *Rev. Geophy.*, 48. doi: 10.1029/2009RG000282.

Haigh JD 2003. The effects solar variability on the earth's climate. *Philos. Trans. R. Soc. London A.*, 361: 95- 111.

Lean J 2006. Comment on estimated solar contribution to the global surface warming using the ARIM TSI satellite composite. *Geophys. Res. lett.*, 33, L15701, doi:10.1029/2005GL025342.

Liu PC & Babanin AV 2004. Using wavelet spectrum analysis to resolve breaking events in the wind wave time series. *Annales Geophysicae*, 22: 3335–3345.

Lockwood M 2010. Solar change and climate: an update in the light of the current exceptional solar minimum. *Proc. R. Soc.*, 466: 303-329. dio: 0.1098/rspa.2009.0519.

Ogunsua BO, Laoye JA, Fuwape IA & Rabiu AB 2014. The comparative study of chaoticity and dynamical complexity of the low-latitude ionosphere, over Nigeria, during quiet and disturbed days. *Nonlin Process Geophys*., 21: 127–142.

Oludehinwa IA, Olusola OI, Bolaji OS & Odeyemi OO 2014. Investigation of nonlinearity effect during storm time disturbance. *Adv. Space Res*., 62: 440–456.

Provenzale A, Smith LA, Vio R & Murante G 1992. Distinguishing between low dimensional dynamics and randomness in measured time series. *Physica* D, 58: 31–49.

Sarp V, Kilcik AA, Yurchyshyn V, Rozelot JP & Ozguc A 2018. Prediction of solar cycle 25: A non-linear approach. *MNRAS*, 481: 2981–2985.

Shaw R 1981. Strange attractors, chaotic behaviour, and information flow. *Z Naturforsch*. 36A: 80.

Takens F 1981. Detecting strange attractors in turbulence. In: Rand D A, Young L S, editor. Lecture Notes in Mathematics, vol. 898, Berlin, Germany: Springer-Verlag, pp. 366 –81.

Torrence C & Compo GP 1998. A practical guide to wavelet analysis. *Bull. Amer. Meteorol. Soc.*, 79: 61–78.

Wallot S & Mønster D 2018. Calculation of average mutual information (AMI) and false-nearest neighbors (FNN) for the estimation of embedding parameters of multidimensional time series in Matlab. *Frontiers in Psychology*, 9: 1679.

Wolf A, Swift JB, Swinney HL &Vastano A 1985. Determining Lyapunov exponents from a time series. *Physica* D, 16: 285–317.

Zossi de Artigas M, Fernandez de Campra P & Zotto EM 2008. Geomagnetic disturbances analysis using discrete wavelets. *Geofísicainternacional*, 47(3): 257-263.